

RESEARCH PAPER



## The long noncoding RNA CRAL reverses cisplatin resistance via the miR-505/CYLD/AKT axis in human gastric cancer cells

Zhangding Wang<sup>a,b,\*</sup>, Qiang Wang<sup>c\*</sup>, Guifang Xu<sup>a\*</sup>, Na Meng<sup>d\*</sup>, Xinli Huang<sup>c</sup>, Zerun Jiang<sup>b</sup>, Chen Chen<sup>b</sup>, Yan Zhang<sup>c</sup>, Junjie Chen<sup>b</sup>, Aiping Li<sup>b</sup>, Nan Li<sup>e</sup>, Xiaoping Zou<sup>a</sup>, Jianwei Zhou<sup>b,f</sup>, Qingqing Ding<sup>g</sup>, and Shouyu Wang<sup>b,c,f,h</sup>

<sup>a</sup>Department of Gastroenterology, The Affiliated Drum Tower Hospital of Nanjing University Medical School, Nanjing, Jiangsu Province, People's Republic of China; <sup>b</sup>Department of Molecular Cell Biology and Toxicology, Key Laboratory of Modern Toxicology of Ministry of Education, School of Public Health, Nanjing Medical University, Nanjing, Jiangsu Province, People's Republic of China; <sup>c</sup>Department of Hepatobiliary Surgery, The Affiliated Drum Tower Hospital of Nanjing University Medical School, Nanjing, Jiangsu Province, People's Republic of China; <sup>d</sup>Department of Medical Records and Statistics, The Affiliated Drum Tower Hospital of Nanjing University Medical School, Nanjing, Jiangsu Province, People's Republic of China; <sup>e</sup>Department of Gastroenterology, Zhongda Hospital Affiliated to Southeast University, Nanjing, Jiangsu Province, People's Republic of China; <sup>f</sup>Jiangsu Key Lab of Cancer Biomarkers, Prevention and Treatment, School of Public Health, Nanjing Medical University, Nanjing, Jiangsu Province, People's Republic of China; <sup>g</sup>Department of Geriatric Oncology, The First Affiliated Hospital of Nanjing Medical University, Nanjing, Jiangsu Province, People's Republic of China; <sup>h</sup>Jiangsu Key Laboratory of Molecular Medicine, Nanjing University Medical School, Nanjing, Jiangsu Province, People's Republic of China

### ABSTRACT

Emerging evidence has suggested that long noncoding RNAs (lncRNAs) play an essential role in the tumorigenesis of multiple types of cancer including gastric cancer (GC). However, the potential biological roles and regulatory mechanisms of lncRNA in response to cisplatin, which may be involved in cisplatin resistance, have not been fully elucidated. In this study, we identified a novel lncRNA, cisplatin resistance-associated lncRNA (CRAL), that was downregulated in cisplatin-resistant GC cells, impaired cisplatin-induced DNA damage and cell apoptosis and thus contributed to cisplatin resistance in GC cells. Furthermore, the results indicated that CRAL mainly resided in the cytoplasm and could sponge endogenous miR-505 to upregulate cylindromatosis (CYLD) expression, which further suppressed AKT activation and led to an increase in the sensitivity of gastric cancer cells to cisplatin *in vitro* and in preclinical models. Moreover, a specific small molecule inhibitor of AKT activation, MK2206, effectively reversed the cisplatin resistance in GC caused by CRAL deficiency. In conclusion, we provide the first evidence that a novel lncRNA, CRAL, could function as a competing endogenous RNA (ceRNA) to reverse GC cisplatin resistance via the miR-505/CYLD/AKT axis, which suggests that CRAL could be considered a potential predictive biomarker and therapeutic target for cisplatin resistance in gastric cancer.

### ARTICLE HISTORY

Received 18 March 2019  
Revised 10 December 2019  
Accepted 12 December 2019

### KEYWORDS

Cisplatin; Gastric cancer; CRAL; CYLD; Drug resistance





### Introduction

Gastric cancer (GC) is the fifth most common malignancy and the second leading cause of cancer death worldwide [1–3]. Chemotherapy is still the main treatment method for patients with advanced stage cancer. Cisplatin is an effective broad-spectrum anticancer drug used in first-line cancer treatment for several types of cancer including GC [4,5]. However, owing to intrinsic or acquired drug resistance, relapse and metastasis are common and result in the high mortality of GC [6]. Therefore, there is an urgent need to elucidate the mechanism of cisplatin resistance in GC.


To date, many molecular mechanisms of drug resistance have been investigated, including increased drug efflux, altered drug metabolism, enhanced DNA repair, and activation of downstream or parallel signalling pathways [7], but the role of potential networks between

mRNAs and noncoding RNAs (ncRNAs) has not been fully elucidated [8]. Among these ncRNAs, long noncoding RNAs (lncRNAs) have attracted the interest of many researchers and become a focus of attention. lncRNAs are known to have many functions, such as acting as scaffolds to regulate interactions between proteins and genes, as decoys to bind miRNAs or proteins, or as enhancers to modulate transcription of their targets [9–13]. Interestingly, accumulating studies have suggested that lncRNAs function as a sponge of miRNAs and contribute to the carcinogenesis, progression, and metastasis of GC and other tumours [14–19]. However, the potential role of lncRNAs as ceRNAs in cisplatin-resistant GC remains unclear.

Here, we established a regulatory ceRNA network related to cisplatin resistance and found a novel lncRNA, termed as CRAL, which was reduced in cisplatin-resistant GC cells. Overexpression of CRAL could reverse cisplatin-induced

**CONTACT** Shouyu Wang  [sywang@nju.edu.cn](mailto:sywang@nju.edu.cn)  Department of Hepatobiliary Surgery, The Affiliated Drum Tower Hospital of Nanjing University Medical School, Nanjing 210000, Jiangsu Province, People's Republic of China; Qingqing Ding  [helen.jsnj@njmu.edu.cn](mailto:helen.jsnj@njmu.edu.cn)  Department of Geriatric Oncology, The First Affiliated Hospital of Nanjing Medical University, Nanjing 210029, Jiangsu Province, People's Republic of China

\*These authors contributed equally to this work

 Supplemental data for this article can be accessed [here](#).

DNA damage and apoptosis. Subsequent mechanistic studies indicated that CRAL exerted its function by competitively sponging miR-505 to augment CYLD expression, which inhibits the activation of PI3K/AKT signalling. Furthermore, the effects of CRAL deficiency could be blocked by a PI3K/AKT-specific inhibitor. In conclusion, our data demonstrated that CRAL could serve as an effective candidate prognostic biomarker for cisplatin resistance and identified a putative drug target for reversing cisplatin resistance in GC.

## Results

### CeRNA networks in cisplatin-resistant GC cells were constructed

To identify differentially expressed lncRNAs and miRNAs, which could be used as potential biomarkers for cisplatin resistance, and elucidate the regulatory networks of

lncRNAs, miRNAs and mRNAs in cisplatin-resistant GC, we analysed two cisplatin-resistant GC cell lines (BGC823/DDP and SGC7901/DDP) and their parental cells (BGC823 and SGC7901) using the Arraystar Human lncRNA microarray V2.0 together with the Affymetrix Human MicroRNA microarray (Fig. 1A). The candidate lncRNAs/mRNAs and miRNAs were selected based on the following criteria: (1) both the ratios of BGC823/DDP to BGC823 and SGC7901/DDP to SGC7901 were  $\geq 2$  or  $\leq 0.5$ ; (2) the miRNAs could predictively interact with lncRNAs and mRNAs; (3) the lncRNAs/mRNAs were upregulated while the miRNAs were downregulated, or the lncRNAs/mRNAs were downregulated while the miRNAs were upregulated (Fig. 1A). The ceRNA networks were then constructed (Supplementary Figure S1A, B). The candidate ceRNA networks in two pairs of cisplatin-resistant GC cells overlapped; three candidate ceRNA clusters were presented, including 8 lncRNAs and 4 mRNAs with low expression levels, and 4 miRNAs with high

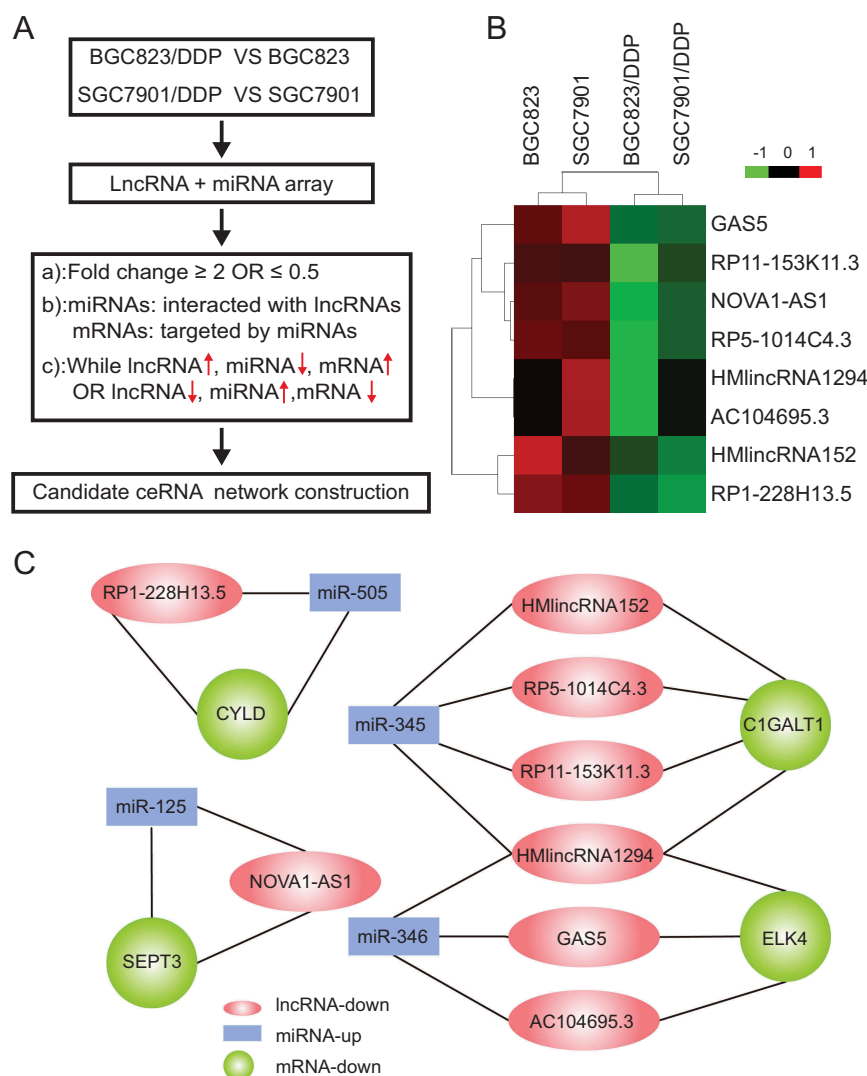


**Figure 1.** The construction of a cisplatin resistance related competing endogenous RNA (ceRNA) network.

A, flowchart of the cisplatin resistance-related ceRNA network using the human lncRNA/mRNA Array v3 and Affymetrix microRNA Array. B, heat map showing 8 candidate lncRNAs that were differentially expressed between the BGC823/DDP and SGC7901/DDP cells and their parental cells. Red indicates upregulation; Green indicates downregulation. C, the ceRNA networks containing upregulated miRNAs and downregulated lncRNAs and mRNAs were constructed.

expression levels in cisplatin-resistant GC cells compared with their counterparts (Fig. 1B, C). Moreover, using the differentially expressed mRNAs as the input, we analysed their biological functions using Gene Ontology (GO) analysis. We found that cell proliferation and apoptotic processes were enriched (Supplementary Figure S1C), which is consistent with our previous studies [20], suggesting that cisplatin-induced cell death may be mainly involved in cisplatin resistance.

To confirm the reliability of the candidate ceRNA networks, we verified the expression of these candidates in two cisplatin-resistant GC cells lines and their parental cells lines via qRT-PCR analysis. Three lncRNAs (RP5-1014C4.3, RP1-228H13.5 and NOVA1-AS1) were significantly downregulated in the BGC823/DDP and SGC7901/DDP cells compared to those in the BGC823 and SGC7901 cells (Fig. 2A, B). In addition, the levels of two miRNAs (miR-125 and miR-505) were higher in the BGC823/DDP and SGC7901/DDP cells than in their counterparts (Fig. 2C, D). Consistently, the mRNA expressions levels of all four candidates were downregulated in the cisplatin-resistant GC cells (Fig. 2E, F). These data suggested that the NOVA1-AS1-miR-125-SEPT3 and RP1-228H13.5-miR-505-CYLD networks may contribute to cisplatin resistance in GC.

### CRAL enhances cisplatin-induced cell death through regulation of DNA damage-induced apoptosis in GC cells

To investigate whether lncRNA NOVA1 and RP1-228H13.5 could modulate the sensitivity of GC cells to cisplatin, we

transfected the BGC823 cells with siRNAs specifically targeting these molecules, and the expression levels of NOVA1 and RP1-228H13.5 were substantially decreased (Supplementary Figure S2A and Fig. 3A). Then, colony formation assays were conducted, and we found that the colony numbers were significantly increased in the RP1-228H13.5-deficient BGC823 cells treated with 0.4 and 0.8  $\mu\text{g/ml}$  cisplatin (Fig. 3B,C), whereas they were not changed in the NOVA1-AS1-deficient BGC823 cells (Supplementary Figure S2B, C) compared with their corresponding control cells. Additionally, to further explore the function of RP1-228H13.5 in cisplatin resistance, we constructed BGC823/DDP cells with stable overexpression of RP1-228H13.5 and the corresponding control cells (Supplementary Figure S2D). The colony numbers were significantly decreased by treatment with 5 and 10  $\mu\text{g/ml}$  cisplatin in the RP1-228H13.5-overexpressing BGC823/DDP cells (Supplementary Figure S2E, F). These data revealed that RP1-228H13.5 may play a critical role in the cisplatin resistance of GC cells; thus, we referred to it in this study as CRAL (Cisplatin Resistance-Associated lncRNA).

In addition, a terminal deoxynucleotidyl transferase-mediated dUTP nick end labelling (TUNEL) assay was used to examine whether CRAL affected cisplatin-induced apoptosis. The apoptotic rate was significantly decreased by treatment with 0.8  $\mu\text{g/ml}$  cisplatin for 48 h in the CRAL-silenced BGC823 cells (Fig. 3D,E). The results were also confirmed by the Annexin-V-FITC/PI assay for detection of apoptotic cells (Fig. 3F,G). The apoptotic rate was significantly increased by treatment with 5  $\mu\text{g/ml}$  cisplatin for 48 h in the CRAL-overexpressing BGC823/DDP cells (Supplementary Figure

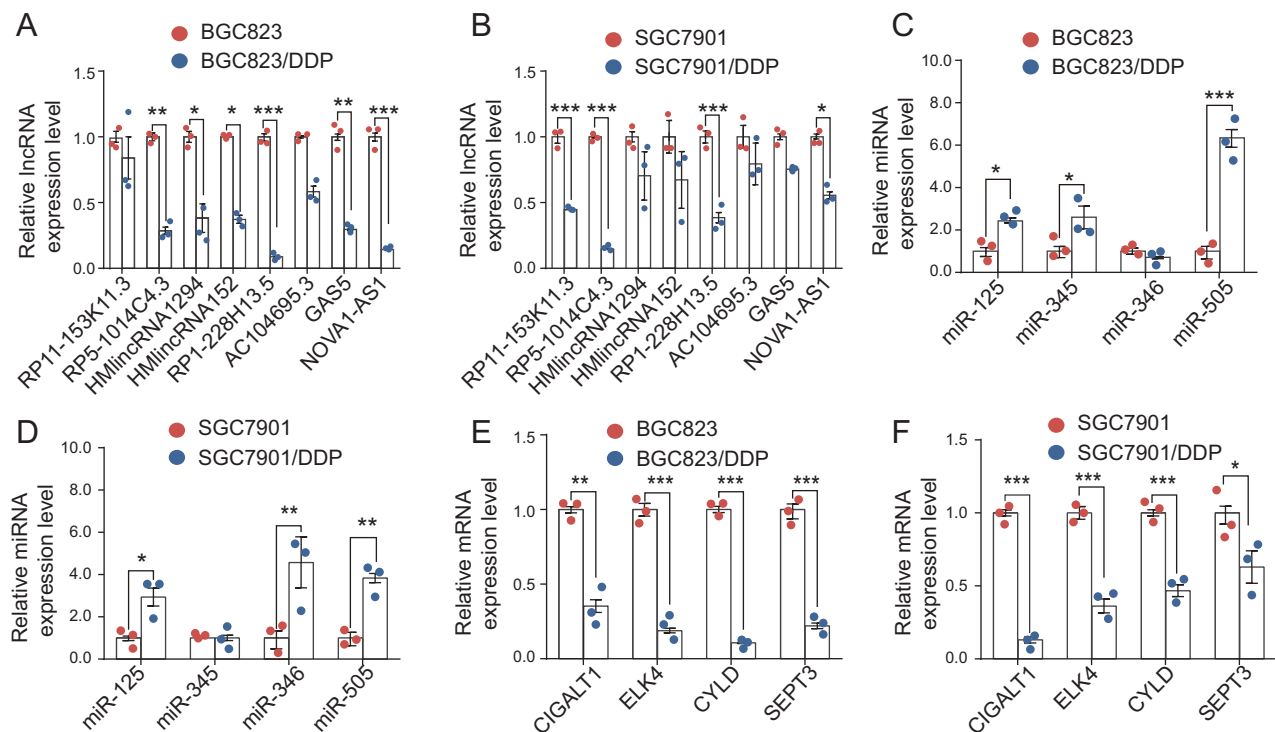


**Figure 2.** Validation of the candidate genes in the ceRNA network. The expression of 8 lncRNAs.

The expression of the candidate lncRNAs (A and B), miRNAs (C and D) and mRNAs (E and F) in the BGC823/DDP cells, SGC7901/DDP cells and their parental counterparts were validated by qRT-PCR. The relative expression level of each gene was normalized by the respective internal reference genes. The data are the mean  $\pm$  SD of three independent experiments. \* $P < 0.05$ ; \*\* $P < 0.01$ ; \*\*\* $P < 0.001$ .

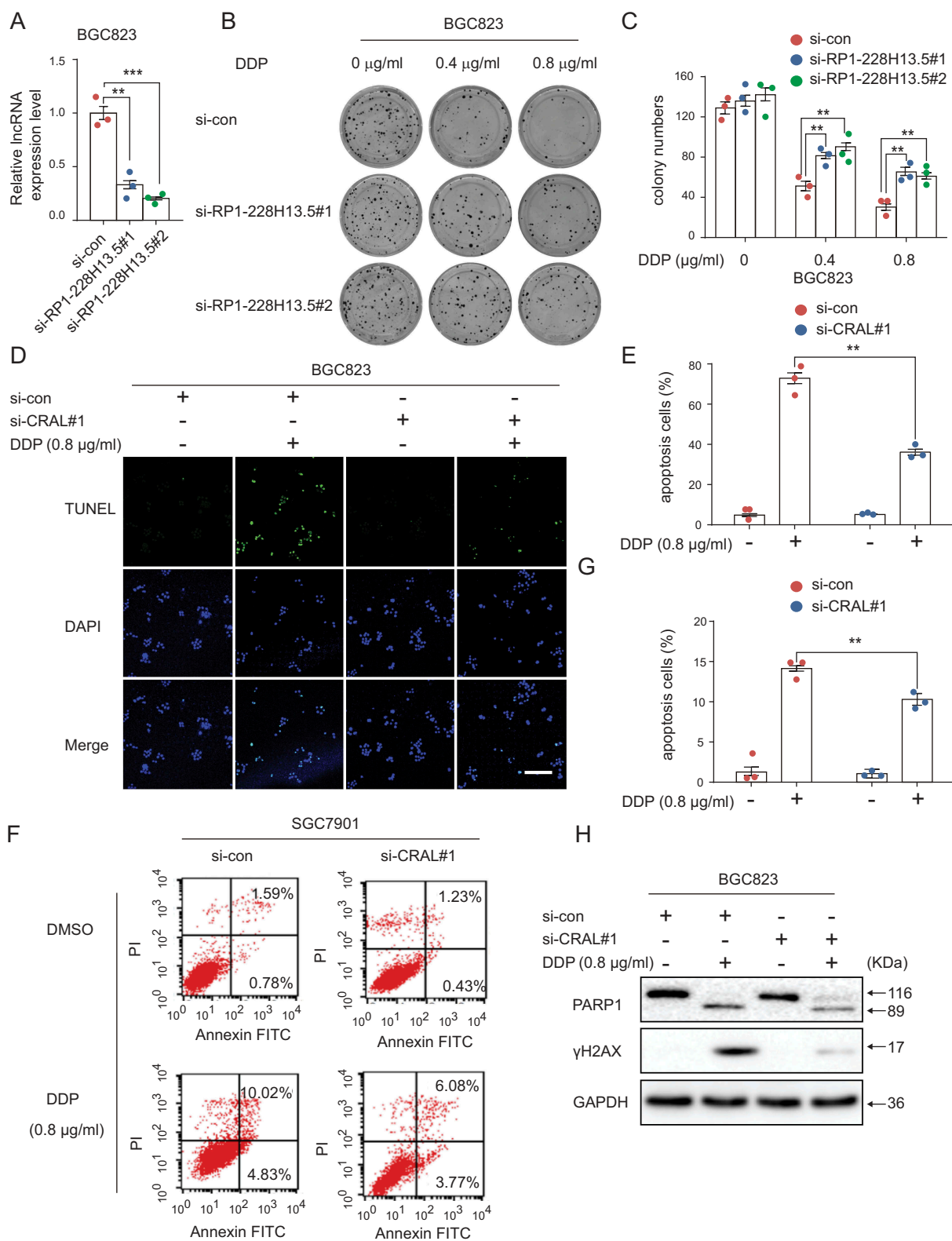


**Figure 3.** CRAL depletion promotes cisplatin resistance in gastric cancer cells.

A, the expression level of RP1-228H13.5 in the BGC823 cells transfected with two specific CRAL siRNAs or control siRNA were determined by qRT-PCR. B, the clonogenic survival assay was performed using the BGC823 cells transfected with RP1-228H13.5 siRNAs or control siRNA, and then treated with or without 0.4 or 0.8  $\mu$ g/ml cisplatin for 2 h. C, the colony numbers in each group were quantified, each colony containing > 50 cells was counted. D, BGC823 cells transfected with CRAL siRNA or control siRNA for 48 h followed by exposure to 0.8  $\mu$ g/ml cisplatin for 48 h were assessed, and the cell death rate was determined by TUNEL assays. Scale bar = 50  $\mu$ m. E, quantification of TUNEL-positive cells in D. F, apoptotic cells were identified by the annexin-V-FITC/PI assay. G, Quantification of the apoptotic cells in F. H, Western blot was applied to determine the expression of  $\gamma$ H2AX and PARP1 in the BGC823 cells under the indicated conditions. The data are the mean  $\pm$  SD of three independent experiments. \*\* $p < 0.01$ ; \*\*\* $p < 0.001$ .

S2G, H). Moreover, the protein levels of phosphorylated histone H2AX ( $\gamma$ H2AX), a sensitive surrogate marker of DSB, and the cleaved form (89 KDa) of poly(ADP-ribose) polymerase 1 (PARP1), a biomarker of apoptosis, were detected.  $\gamma$ H2AX and the cleaved form of PARP1 were significantly decreased in the CRAL knockdown BGC823 cells treated with 0.8  $\mu$ g/ml cisplatin for 48 h (Fig. 3H), but increased in the CRAL-overexpressing BGC823/DDP cells treated with 5  $\mu$ g/ml cisplatin for 48 h (Supplementary Figure S2I) compared with their corresponding controls. These results suggest that loss of CRAL expression in GC cells inhibited

cisplatin-induced DNA damage and apoptosis, which may lead to cisplatin resistance in GC cells.

### CRAL serves as a sponge for miR-505 to regulate cisplatin resistance

The subcellular localization of lncRNA will affect their functions in cells [21,22]. Thus, we examined CRAL expression in the cytoplasmic and nuclear RNA fractions using qRT-PCR analysis and found that CRAL mainly resided in the

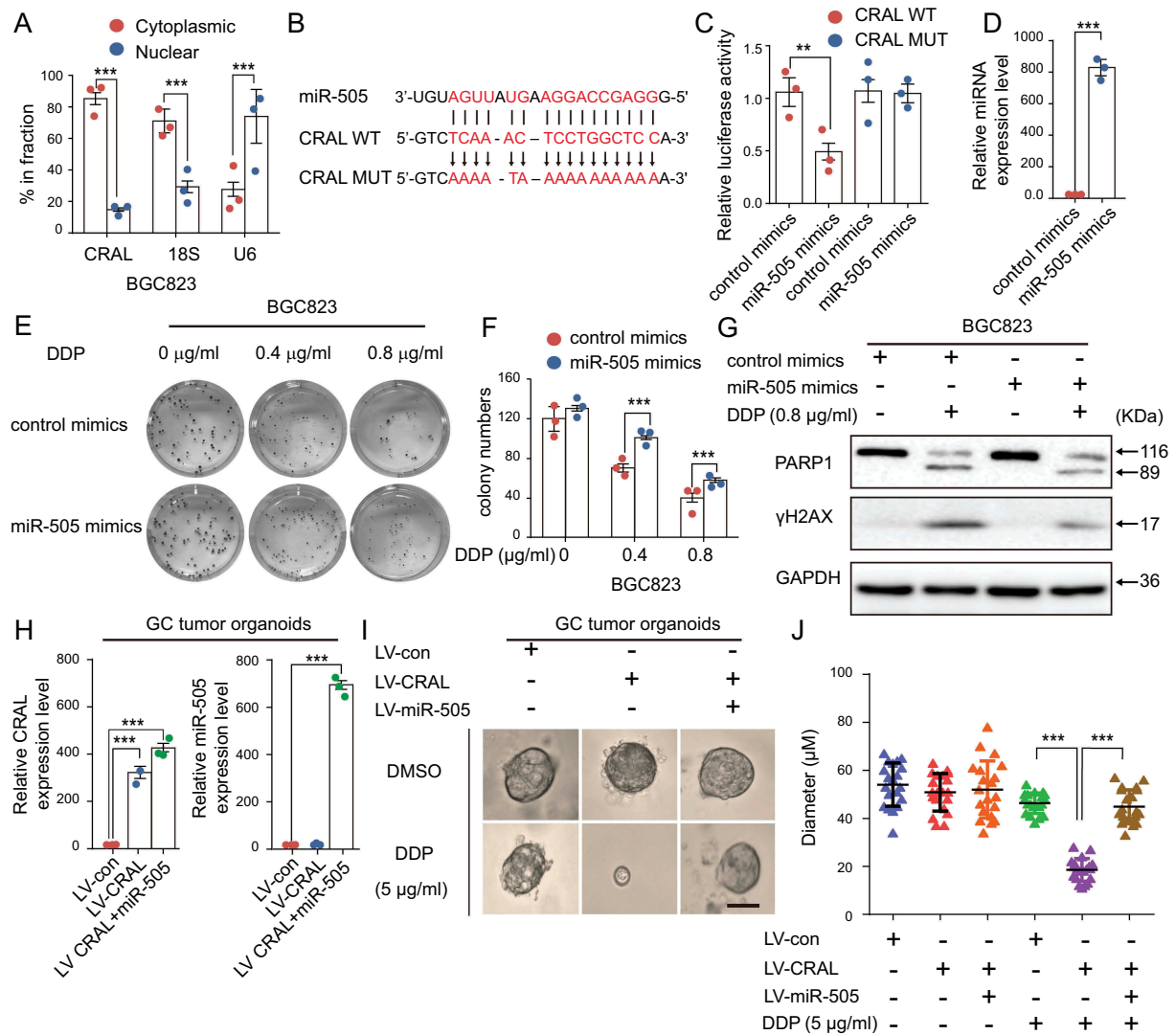


**Figure 4.** miR-505 interacts with CRAL and enhances cisplatin resistance in GC cells.

A, nuclear and cytoplasmic fractions were isolated to detect the localization of CRAL in BGC823 cells. U6 was used as a positive control for the nuclear fractions, 18S rRNA was used as a positive control for the cytoplasmic fractions. B, schematic graph illustrating the potential binding sites between miR-505 and CRAL (WT or Mutant). C, the luciferase reporter assay was used to detect the luciferase activity of LUC-CRAL or LUC-CRAL mutants in the BGC823 cells cotransfected with miR-505 mimics or the corresponding control. Data are presented as the relative ratio of renilla luciferase activity and firefly luciferase activity. D, relative expression level of miR-505 in the BGC823 cells transfected with the mimic control or miR-505 mimic was detected by qRT-PCR. E, BGC823 cells were transfected with miR-505 mimics or mimic control for 48 h and then subjected to clonogenic survival assays for 2 weeks after treatment with cisplatin for 2 h. F, quantification of the numbers of colonies in E. G, Western blotting was applied to determine the expression of  $\gamma$ H2AX and PARP1 in the BGC823 cells under the indicated conditions. H, Relative expression levels of CRAL and miR-505 in the GC organoids transfected with CRAL or miR-505-overexpressing lentiviral plasmids. I, GC organoids were transfected with LV-CRAL or LV-miR-505 and the corresponding control lentiviral vectors for 8 h. Then, the organoids were seeded into 24-well plates for 2 weeks with or without cisplatin treatment (5  $\mu$ g/ml). J, quantitative analysis of the organoid images. Scale bar = 50  $\mu$ m. The data are the mean  $\pm$  SD of three independent experiments. \*\*P < 0.01; \*\*\*P < 0.001.

cytoplasm (Fig. 4A). Moreover, CRAL was also high abundant in the BGC823 and SGC7901 cells compared with several well-known and highly expressed oncogenic lncRNAs (such as HOTAIR [23,24] and MALAT1 [25–27]) in gastric cancer (Supplementary Figure S3A). Based on the ceRNA network described in Fig. 1C, CRAL may exert its function in the cytoplasm through sponging miR-505. Considering that the expression level of miR-505 was higher in the cisplatin-resistant GC cells than in their parental cells, we examined the miR-505 levels in the CRAL-deficient BGC823 cells or the CRAL-overexpressing BGC823/DDP cells and their corresponding controls. We found that the miR-505 levels were not affected (Supplementary Figure S3B, C).

Further, to examine whether miR-505 could bind to CRAL, the sequence of CRAL was analysed using an online bioinformatics database (DIANA Tools) and found that CRAL contains a potential miR-505 binding site (Fig. 4B). To further assess the interaction of CRAL and miR-505, we inserted the sequences with wild-type (CRAL WT) or mutated potential binding sites (CRAL MUT) into a luciferase reporter vector (Fig. 4B). We found that the transfection of miR-505 mimics significantly inhibited the luciferase activity of the CRAL WT reporter, whereas this effect was completely abolished for CRAL MUT reporter (Fig. 4C), indicating that CRAL may function as a sponge to bind with miR-505.

To investigate whether miR-505 is involved in modulating cisplatin resistance in GC cells, we transfected the BGC823 and BGC823/DDP cells with miR-505 mimics (Fig. 4D) or miR-505 inhibitor (Supplementary Figure S3D), respectively. We found that the colony numbers were significantly increased in miR-505-overexpressing BGC823 cells following treatment with 0.4 or 0.8  $\mu\text{g/ml}$  cisplatin (Fig. 4E,F), which was also confirmed in the cells stably overexpressing miR-505 (LV-miR-505) (Supplementary Figure S3E-G). In contrast, significantly decreased colony numbers were observed following treatment with 5 or 10  $\mu\text{g/ml}$  cisplatin in the miR-505 knockdown BGC823/DDP cells (Supplementary Figure S3H, I) compared with their corresponding controls. Moreover, the cleaved forms of PARP1 and the  $\gamma\text{H2AX}$  levels were significantly reduced in the miR-505-overexpressing BGC823 cells treated with 0.8  $\mu\text{g/ml}$  cisplatin for 24 h (Fig. 4G) but increased in the miR-505-deficient BGC823/DDP cells treated with 5  $\mu\text{g/ml}$  cisplatin for 24 h (Supplementary Figure S3J) compared with their counterparts.

To further examine the roles of CRAL and miR-505 in cisplatin-resistant GC cells, we established a preclinical organoid model. The diameter of CRAL-overexpressing tumour organoids was smaller than those in their counterparts after treatment with 5  $\mu\text{g/ml}$  cisplatin, but these effects were reversed upon overexpression of miR-505 in these tumour organoids (Fig. 4H,I,J). Collectively, these results suggest that CRAL serves as a ceRNA for miR-505, which could impede cisplatin-induced DNA damage and apoptosis.

#### **CYLD is a miR-505 target gene and enhances cisplatin sensitivity of GC cells**

The CRAL-miR-505-CYLD network has been identified and may contribute to cisplatin resistance in GC cells (Fig. 1C),

prompting us to investigate whether CRAL-miR-505 could regulate CYLD expression and reverse cisplatin resistance via CYLD. Intriguingly, Western blot analysis showed that the CYLD protein levels in two pairs of cisplatin-resistant GC cells (BGC823/DDP and SGC7901/DDP) were substantially decreased compared with those of parental cells (Fig. 5A). Moreover, the miR-505 mimics significantly suppressed, but the miR-505 inhibitor dramatically enhanced, the CYLD protein levels in the BGC823 cells and BGC823/DDP cells, respectively (Fig. 5B). Then, BGC823 cells were transfected with CYLD-specific siRNAs to knock down the expression of this molecule, which was confirmed by Western blot (Fig. 5C). The long-term clonogenic survival assay showed that CYLD knockdown significantly increased the colony numbers of the BGC823 cells after treatment with 0.4 or 0.8  $\mu\text{g/ml}$  cisplatin (Fig. 5D,E). Meanwhile, the cleaved PARP1 and  $\gamma\text{H2AX}$  levels were significantly decreased in the CYLD-deficient BGC823 cells after treatment with 0.8  $\mu\text{g/ml}$  cisplatin (Fig. 5F). In contrast, overexpression of CYLD significantly inhibited the colony formation of the BGC823/DDP cells treated with 5 or 10  $\mu\text{g/ml}$  cisplatin (Supplementary Figure S4A-C). Accordingly, significantly increased  $\gamma\text{H2AX}$  levels and cleaved PARP1 levels were observed in the CYLD-overexpressing BGC823/DDP cells after treatment with 5  $\mu\text{g/ml}$  cisplatin compared with the control cells (Supplementary Figure S4D). Taken together, these results indicated that CYLD may enhance cisplatin-induced DNA damage and apoptosis in GC cells.

#### **CRAL modulates cisplatin resistance via regulating CYLD expression**

To assess whether CRAL-enhanced cisplatin-induced apoptosis and DNA damage via regulation of the miR-505/CYLD axis, we first examined CYLD expression in the CRAL-deficient BGC823 cells or CRAL-overexpressing BGC823/DDP cells. The expression of CYLD was significantly decreased in the CRAL knockdown cells but increased in the CRAL-overexpressing cells, compared with their corresponding controls (Fig. 6A). Intriguingly, the colony numbers were decreased in the CRAL-overexpressing BGC823/DDP cells treated with cisplatin, but this effect was significantly inhibited by knockdown of CYLD in these cells (Fig. 6B-D). In addition, TUNEL assays showed that knockdown of CYLD could suppress the CRAL-induced apoptosis in the BGC823/DDP cells treated with 5  $\mu\text{g/ml}$  cisplatin (Fig. 6E,F). Overexpression of CRAL increased the levels of the cleaved forms of PARP1 and  $\gamma\text{H2AX}$ , which were reversed by CYLD knockdown in the BGC823/DDP cells treated with 5  $\mu\text{g/ml}$  cisplatin (Fig. 6G). Therefore, these results indicate that CRAL modulates cisplatin resistance in GC cells via regulating CYLD expression.

#### **CRAL depletion promotes cisplatin resistance via activating the PI3K/AKT signalling pathway**

CYLD was reported to negatively regulate PI3K/AKT activation [28,29], which was associated with drug resistance in multiple cancers [30,31]. Intriguingly, based on the KEGG

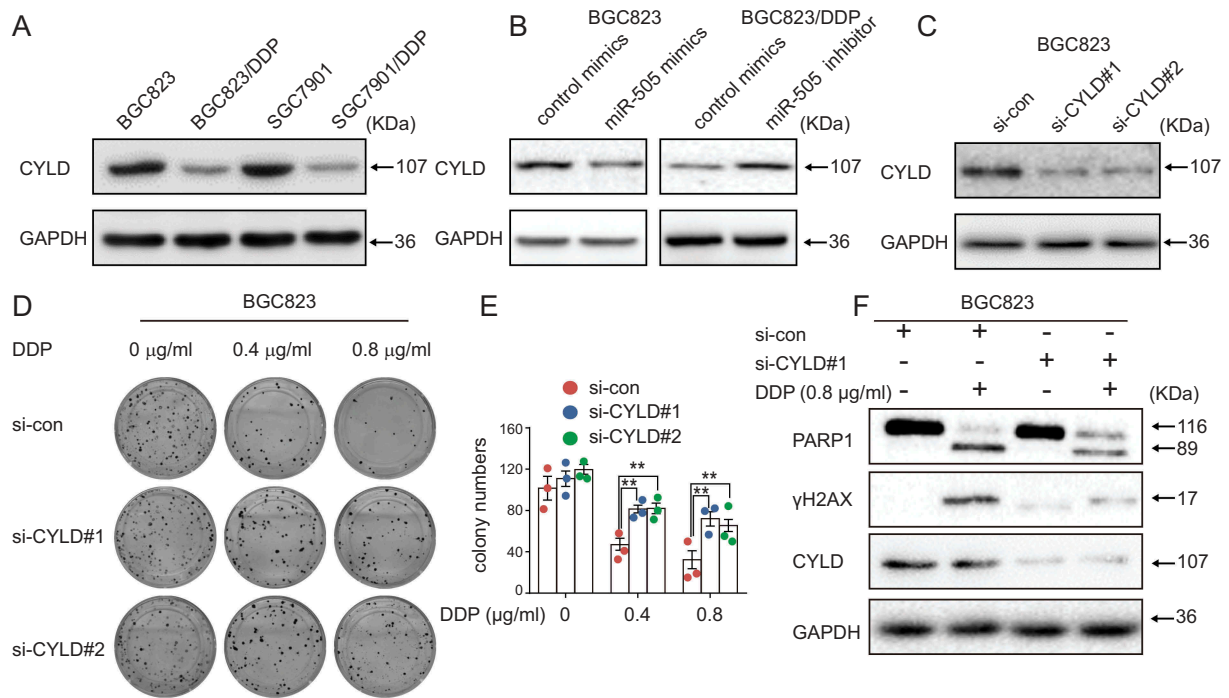


**Figure 5.** CYLD is a target of miR-505 and enhances cisplatin sensitivity of GC cells.

A, Western blotting was used to determine the expression of CYLD in the BGC823/DDP and SGC7901/DDP cells and their corresponding control cells. B, Western blotting was applied to detect the expression of CYLD in the BGC823 cells and BGC823/DDP cells transfected with miR-505 mimics and miR-505 inhibitor or their corresponding controls. C, the expression of CYLD was detected in the CYLD-deficient BGC823 cells. D, BGC823 cells were transfected with specific CYLD siRNAs or control siRNA for 48 h and then subjected to clonogenic survival assays for 2 weeks after treatment with cisplatin for 2 h. E, quantification of the numbers of colonies in D. F, the indicated protein levels were detected by western blotting in the CYLD-deficient BGC823 cells treated with 0.8 µg/ml cisplatin for 24 h. The data are the mean ± SD of three independent experiments. \*\* $P < 0.01$ .

pathway analysis, we observed that AKT activation was also dramatically increased in cisplatin-resistant GC cells (Fig. 7A). As shown in Fig. 7B, we found that the level of AKT phosphorylation in the BGC823/DDP and SGC7901/DDP cells was obviously higher than that in its parental cells (BGC823 and SGC7901 cells, respectively). Therefore, we examined whether the PI3K/AKT signalling pathway was involved in the CRAL/CYLD-mediated cisplatin resistance. Knockdown of CRAL significantly suppressed the CYLD expression and increased the p-AKT level, which were reversed upon overexpression of CYLD in BGC823 cells (Fig. 7C). Furthermore, TUNEL assays showed that cell death was significantly decreased in the CRAL-deficient BGC823 cells treated with 0.8 µg/ml cisplatin for 48h but partly restored in the CRAL-deficient BGC823 cells pretreated with MK2206, a specific small molecule inhibitor of AKT activation (Fig. 7D,E). Consistently, Western blot confirmed that inhibition of AKT activation could significantly re-induce the cleaved forms of PARP1 and γH2AX in the CRAL-deficient BGC823 cells treated with 0.8 µg/ml cisplatin (Fig. 7F).

### CRAL is an independent predictor of GC survival

To further examine the clinical significance of CRAL-miR-505-CYLD network in GC, we used data from The Cancer Genome Atlas (TCGA). We found that miR-505 exhibited a negative correlation with CRAL and CYLD expression in the GC samples, while CRAL expression was positively correlated with the expression of CYLD (Fig. 8A-C).

Moreover, the GC samples were divided into the CRAL high expression ( $n = 113$ ) and low expression ( $n = 38$ ). Kaplan-Meier analysis revealed that the GC patients with low CRAL expression had a shorter survival time than those with high CRAL expression (Fig. 8D). In addition, we found that cervix neoplasia patients with high CRAL expression had a longer survival time than those with low expression, but this effect was not found in hepatocellular carcinoma (Supplementary Figure S5A). Interestingly, a high expression level of miR-505 was a risk factor for the prognosis of patients with GC, although it showed a borderline statistical significance ( $P = 0.056$ ) (Fig. 8E). Furthermore, miR-505 could act as a risk factor for patients with sarcoma, but as a protective factor for the prognosis of patients with bladder carcinoma (Supplementary Figure S5B). Moreover, high CYLD expression was related to a good prognosis in patients with GC, lung adenocarcinoma and breast cancer (Fig. 8F and Supplementary Figure S5C). Taken together, these results indicated that CRAL, miR-505 and CYLD could function as independent predictors of survival for GC patients.

### Discussion

Increasing evidence on the role of lncRNA in chemotherapeutic resistance has been reported. In this study, we used lncRNAs and microRNA arrays to identify the regulatory networks of mRNAs and ncRNAs in cisplatin resistance of GC. We found that a novel lncRNA, CRAL, competitively

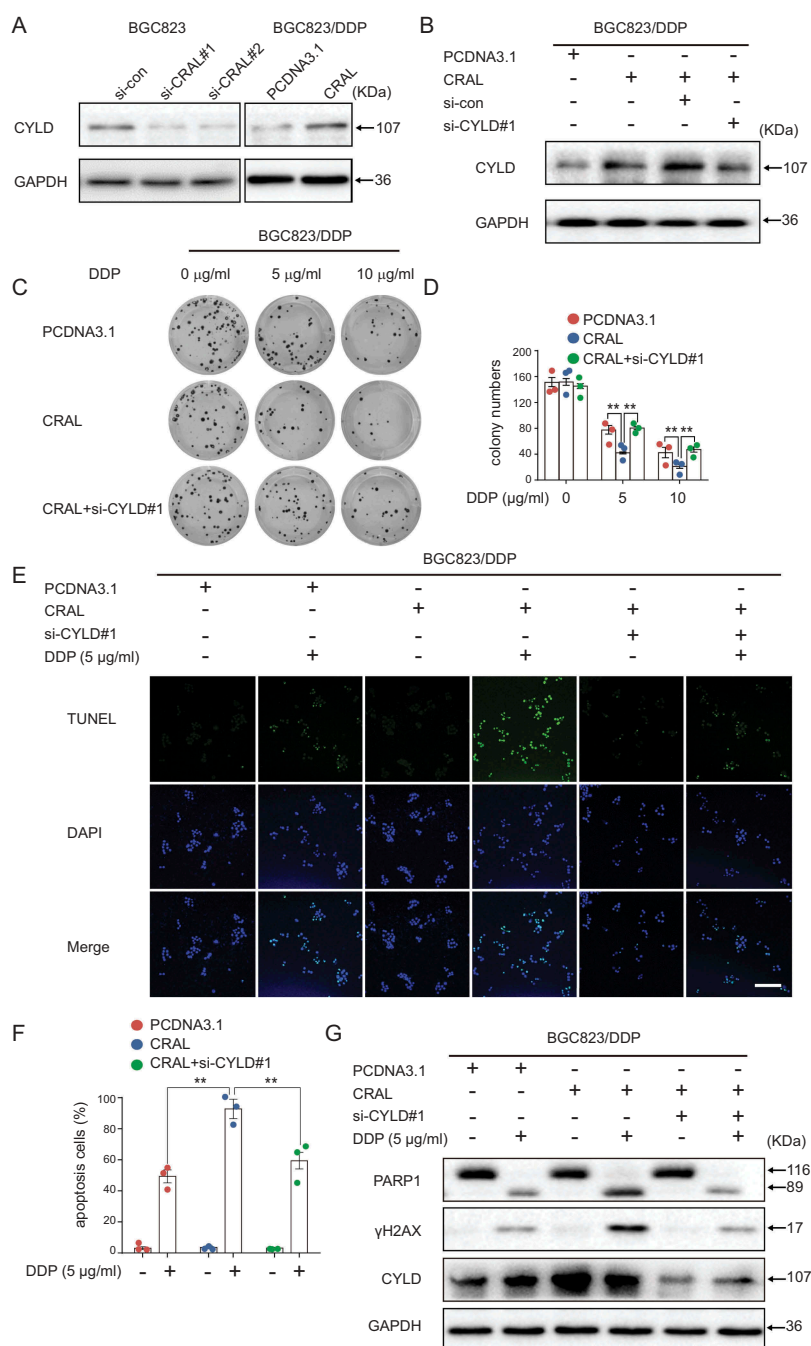


**Figure 6.** CRAL promotes cisplatin-induced apoptosis and DNA damage by regulating CYLD expression.

A, the CYLD expression level was detected by western blotting in the CRAL-deficient BGC823 cells or CRAL-overexpressing BGC823/DDP cells. B, Western blotting was applied to determine the expression of CYLD in the BGC823/DDP cells transfected with a CRAL-overexpression plasmid for 12 h, followed by transfection with the CYLD siRNAs or control siRNAs for 48 h. C, the CRAL-overexpressing BGC823/DDP cells treated with CYLD siRNAs and the corresponding control cells were subjected to clonogenic survival assays 2 weeks after treatment with 0, 5, or 10  $\mu\text{g/ml}$  cisplatin for 2 h. D, quantification of the number of colonies in C. E, TUNEL assays were used to assess the apoptotic cells in the CRAL-overexpressing BGC823/DDP cells transfected with CYLD siRNAs and then treated with 5  $\mu\text{g/ml}$  cisplatin for 24 h, scale bar = 50  $\mu\text{m}$ . F, quantification of the TUNEL-positive cells in E. G, Western blotting was performed to determine the expression of the indicated proteins. The data are the mean  $\pm$  SD of three independent experiments. \*\* $P < 0.01$ .

binds with miR-505, thus upregulating CYLD expression and then suppressing PI3K/AKT signalling, which modulates the cisplatin response in GC cells (Fig. 8F). Intriguingly, we found that an inhibitor of PI3K/AKT signalling could effectively reverse cisplatin resistance in GC cells with low expression of CRAL, which provides new treatment options for GC patients.

Many molecular mechanisms of GC drug resistance are being revealed, and thousands of genes have been shown to play a vital role in this process [20,32]. Genes rarely work alone, and most of them always function through network regulation based on their interactions. A growing body of evidence has shown that lncRNAs are involved in a wide range of biological functions through diverse molecular



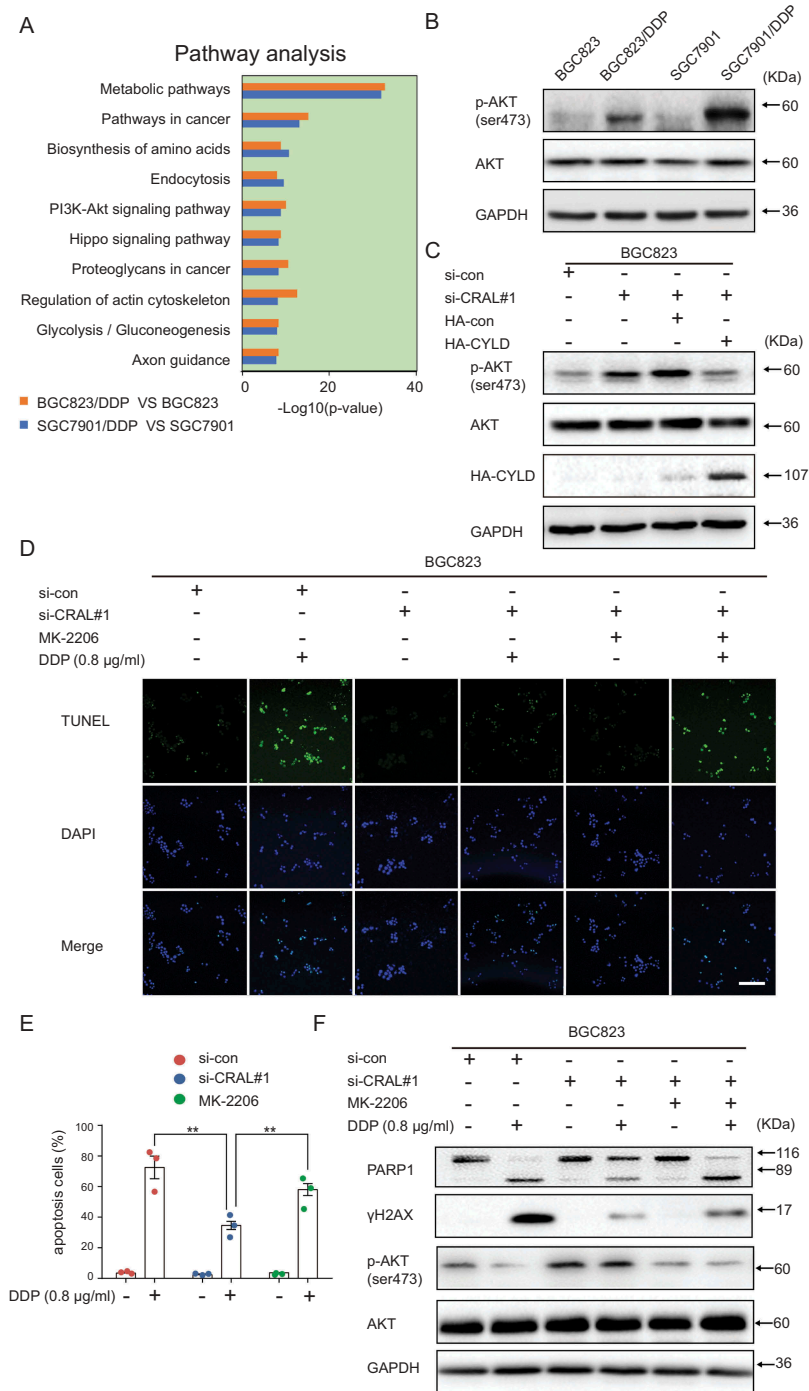


**Figure 7.** CRAL depletion promotes cisplatin resistance via activating CYLD-mediated AKT signalling.

A, KEGG pathway enrichment analysis of differentially expressed genes between the cisplatin-resistant GC cells (BGC823/DDP and SGC7901/DDP) and their counterparts. B, Western blotting was used to determine the activation of AKT in the BGC823/DDP cells, the SGC7901/DDP cells and their counterparts. C, the indicated protein levels were detected in the CRAL-deficient BGC823 cells transfected with the CYLD-overexpressing plasmid and their controls. D, TUNEL assays were performed to assess apoptosis in the CRAL-deficient BGC823 cells treated with AKT inhibitor MK-2206 (5  $\mu\text{M}$ ) for 24 h, followed by exposure to 0.5  $\mu\text{g/ml}$  of cisplatin for 24 h, scale bar = 50  $\mu\text{m}$ . E, quantification of the TUNEL-positive cells in D. F, the expression of  $\gamma\text{H2AX}$  and PARP1 was determined by Western blotting. The data are the mean  $\pm$  SD of three independent experiments. **\*\*** $P < 0.01$ .

mechanisms. Some of them linked to the transcription site to regulate the expression of genes in *cis* [33], while others interact with chromatin-modifying complexes and lead them to their genomic target in *trans* [34]. LncRNAs also function as molecular decoys for miRNAs and modulate their target genes expression [35]. Establishment of a coexpression

network of ceRNAs can be used to predict lncRNA/miRNA functions, as these functions can be deduced from the coding genes (mRNAs) [36,37]. Recent studies have also shown that ceRNAs are widely involved in cancer drug resistance. For example, Cao et al. showed that lncRNA-SNHG6-003 functions as a ceRNA for miR-26 a/b, thereby promoting cell

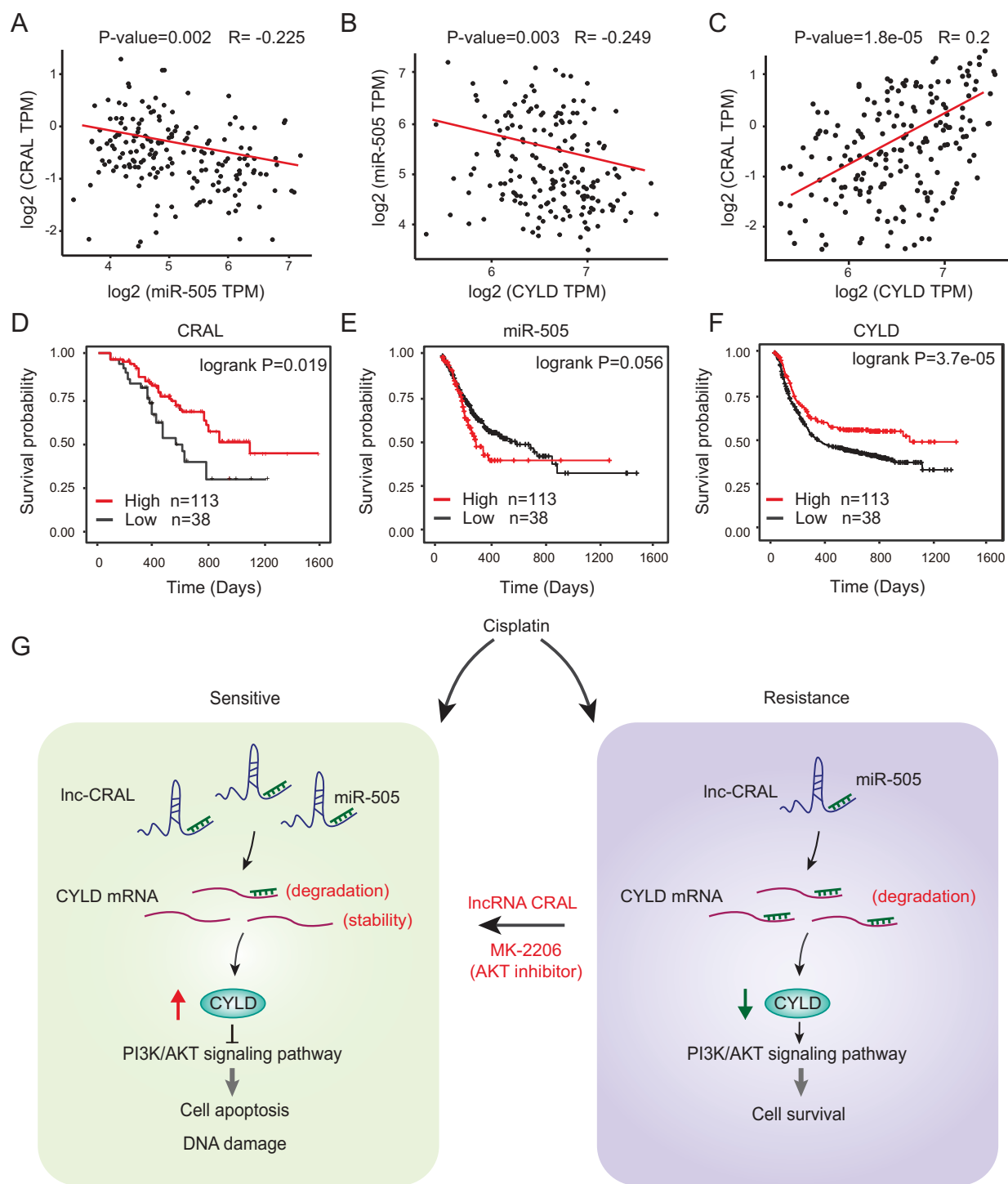


**Figure 8.** CRAL is an independent predictor of GC survival.

A, TCGA data analysis of the correlation of CRAL expression with miR-505 in the gastric cancer samples. B, TCGA data analysis of the correlation of miR-505 expression with CYLD in the GC samples. C, TCGA data analysis of the correlation of CRAL expression with CYLD in the GC samples. D, Kaplan-Meier analysis of the association of CRAL expression with overall survival in the GC patients from TCGA data. E, Kaplan-Meier analysis of the association of miR-505 expression with overall survival in the GC patients from TCGA data. F, Kaplan-Meier analysis of the association of CYLD expression with overall survival in the GC patients from TCGA data. G, a schematic model of CRAL functioning as a decoy by competitively binding miR-505 to prevent its interaction with CYLD and the degradation of CYLD mRNA, which suppresses AKT activation and enhances cisplatin sensitivity in GC cells.

proliferation and inducing drug resistance [38]. Recent evidence has showed that the lncRNA-LET/miR-145 axis could promote gemcitabine resistance in bladder cancer through enhancing cancer cell stemness [39]. Likewise, lncRNA-ARSR can act as a ceRNA for miR-34 and miR-449 to

facilitate AXL and c-MET expression, thus promoting sunitinib resistance in renal cell carcinoma [18]. However, the signature of ceRNAs in the development of cisplatin resistance in GC has not been elucidated. In this report, our data demonstrated that lncRNA-CRAL could function as an

endogenous sponge to bind with miR-505 and modulate CYLD expression, which could reverse cisplatin resistance by increasing cell apoptosis and DNA damage. We also validated CRAL and its clinical functions in a public database and found that CRAL could function as an independent predictor of survival for GC and cervical neoplasia patients. However, the patients with hepatocellular carcinoma and high CRAL expression had a shorter survival time than those with low expression, which was consistent with a previous study [40], suggesting that CRAL may play different roles in multiple types of cancer.

Several studies have reported that miR-505 acts as a tumour suppressor by suppressing tumour growth in hepatocellular carcinoma cells [41] and promoting cell apoptosis in breast cancer cells [42] via targeting different downstream genes. Other recent studies have also demonstrated that miR-505 could suppress GC cell proliferation and invasion [43]. However, Cao et al. showed that miR-505 could mediate MTX (methotrexate) resistance in human colorectal cancer, and downregulation of miR-505 expression weakened the proliferative ability and induced cell cycle arrest and apoptosis [44]. Here, we employed integrated analysis and found that miR-505 is upregulated in cisplatin-resistant GC cells, affecting cisplatin-induced DNA damage and cell apoptosis. By analysing TCGA data, we also found that high miR-505 expressing acted as an oncogene in sarcoma, but in bladder carcinoma, higher miR-505 expression was associated with a better survival rate, which fully demonstrated its role as a tumour suppressor. Taken together, these results indicated that miR-505 may have opposite functions in different tumours and different physiological states.

Several studies have shown constitutively activated PI3K/AKT signalling and upregulation of drug resistance-associated proteins [45–47], such as multidrug resistance 1 (MDR1) and P-glycoprotein (P-gp), in various cancers [48–50]. CYLD, a deubiquitination enzyme, acts as a tumour suppressor in different types of cancer [51–54]. Currently, CYLD is known to function as a negative regulator of the PI3K/AKT/NF- $\kappa$ B signalling pathway and is closely involved in regulating the apoptosis of cancer cells [30,55]. In addition, previous investigations have suggested that inhibition of the PI3K/AKT pathway sensitized cells to chemotherapeutic drugs in gastric cancer [56,57]. Recently, small molecule inhibitors targeting the pleckstrin homology (PH) domains of AKT, e.g., MK2206, have been used in clinical trials for aggressive cancers alone or in combination with other pathway inhibitors, but the clinical effect was disappointing due to toxicity and drug resistance [58]. Here we found that CRAL-deficient GC cells decreased the expression of CYLD and increased the activation of AKT. However, blocking the PI3K/AKT signalling pathway can effectively reverse cisplatin resistance in GC caused by CRAL deficiency. Therefore, GC patients could be stratified based on the CRAL expression levels to help determine the suitability of an individual for AKT inhibitor treatment.

In summary, we provide the first evidence that a novel lncRNA, CRAL, could function as a ceRNA to reverse GC

cisplatin resistance via the miR-505/CYLD/AKT axis, which suggests that CRAL could be a potential predictive biomarker and therapeutic target for cisplatin resistance in gastric cancer in the future.

## Materials and methods

### Cell culture and reagents

The cells used in this study consisted of four cell lines, two cisplatin-sensitive GC cells BGC823 and SGC7901 and their parent cisplatin-resistant GC cell lines BGC823/DDP and SGC7901/DDP. BGC823 and SGC7901 cells were purchased from the Type Culture Collection of the Chinese Academy of Sciences (Shanghai, China). The cells were cultured with 5% CO<sub>2</sub> in RPMI 1640, supplemented with 100 U/ml penicillin, 100  $\mu$ g/ml streptomycin and 10% foetal bovine serum. AKT inhibitor MK-2206 was purchased from CSNpharm (CSN15705, USA), Cisplatin was purchased from SelleckChem (Houston, TX, USA). The BGC823/DDP and SGC7901/DDP cells were developed by chronic, repeated exposure to cisplatin, as described in our previous studies [20,59]. For all experiments, the cisplatin-resistant cells were cultured in drug-free RPMI 1640 medium for 2 weeks.

### Microarray analysis

Microarray analysis was conducted to compare the differentially expressed lncRNAs, miRNAs and mRNAs between the cisplatin sensitive GC cells and cisplatin-resistant cells. The human lncRNA/mRNA Array v3.0 was utilized to analyse the lncRNA and mRNA profiles, and the Affymetrix GeneChip miRNA 2.0 Array was used to analyse the miRNA profiles. Candidate genes with a fold change  $\geq 2$  or  $\leq 0.5$  were used to construct ceRNA network. The Cluster 3.0 and Tree View programs (Stanford University, CA, USA) were used for visualization.

### Plasmids, siRNA, transfection and lentiviral transduction

The CRAL sequence was synthesized and subcloned into a pCDNA3.1 vector. The HA-con and HA-CYLD plasmids were purchased from Addgene (Addgene Plasmid #22,544). CRAL siRNA, ENST00000548328 siRNA, CYLD siRNA, miR-505 mimics, miR-505 inhibitor and their respective negative controls were synthesized by RiboBio (Guangzhou, China) (sequences of the siRNAs are listed in Supplementary Table 1). Plasmids and miRNA mimics and inhibitors were transfected into cells with Lipofectamine 2000 (Invitrogen), and the siRNAs were transfected into cells with DharmaFECT4 (Dharmacon) according to the manufacturer's instructions.

For lentiviral transduction, virus-containing supernatant was collected 48 h after the cotransfection of packaging plasmids (pCMV-VSV-G and pCMV- $\Delta$ 8.2) and the CRAL-overexpressing or miR-505-overexpressing vector (GV358) into HER-293T cells, followed by its addition to the target

cells. Twenty-four hours later, the infected cells were selected with 2 µg/ml puromycin (Gibco, A11138-03).

### **Quantitative real-time RT-PCR (qRT-PCR) assay**

Total RNAs was extracted from the cells using TRIzol reagent (Invitrogen, Carlsbad, CA, USA) according to the manufacturer's instructions. The reverse transcription reaction (RT) was performed with HiScript Q RT SuperMix for qPCR (Vazyme, Jiangsu, China). The RT-PCR reactions were performed with a SYBR Green PCR Kit (Vazyme, Jiangsu, China), measured in triplicate and performed on an Applied Biosystems 7900HT sequence detection system (Applied Biosystems). GAPDH was used as an internal control for lncRNA and mRNA, and expression levels of U6 were used as a loading control for miRNA. The relative expression levels of the target miRNAs were calculated using the comparative  $2^{-\Delta\Delta C_t}$  method. The quantification of miRNA was performed using the specific primers for the reverse transcription and RT-PCR reactions from the BulgeLoop™ miRNA qRT-PCR Primer Set (RiboBio, China). The primers for the lncRNAs and mRNAs are listed in Supplementary Table 1.

### **Nuclear-cytoplasmic fractionation**

Nuclear/cytoplasmic fractionation was conducted via the Protein and RNA Isolation System (Ambion) according to the manufacturer's protocols. U6 was used as a nuclear control while GAPDH was used as a cytoplasmic control.

### **Western blotting**

The Western blot protocol was performed as previously described [60]. The antibodies used were as follows: anti-CYLD (Proteintech, Wuhan, China); anti-GAPDH and anti-β-actin (Beyotime, Shanghai, China); anti-γH2AX (Abcam, Shanghai, China); anti-PARP1, anti-p-AKT and anti-AKT (Cell Signalling Technology, Massachusetts, USA).

### **Luciferase reporter assay**

Cells were seeded in 24 well plates ( $1 \times 10^5$  cells per well). After 24 h, the cells were transiently cotransfected with 30 ng of CRAL wild-type or mutant constructed pmiR-RB-REPORTTM vectors (the primers of CRAL WT and MUT are listed in Supplementary Table 1), and 50 nM of miR-505 mimics. After 48 h, the luciferase activity was measured with a Dual-luciferase assay kit (Promega). Renilla luciferase activity was normalized to firefly luciferase activity.

### **Cell apoptosis assay**

Apoptosis was assessed using TUNEL Apoptosis Detection Kit (Yeasen, Shanghai, China) according to the manufacturer's instructions. Cell nuclei were stained with DAPI. The confocal images of the cells were sequentially acquired with Zeiss AIM software on a Zeiss LSM 510 confocal microscope system, and the TUNEL-positive cells were counted.

In addition, the Annexin-V-FITC/PI method was used to identify the apoptotic cells. Briefly, the cells were seeded in 24 well plates ( $1 \times 10^5$  cells per well) and then treated with the indicated plasmids, siRNAs and cisplatin for the indicated times. The cells were centrifuged and resuspended in cold binding buffer. One hundred microliters of the sample solution were transferred to a 5 ml culture tube and incubated with 5 µl of FITC-conjugated Annexin V and 5 µl of PI for 15 mins at room temperature in the dark. Four hundred microliters of binding buffer were added to each sample tube and subjected to a FACS Calibur flow cytometer (Becton Dickinson, CA, USA). The results were analysed by CellQuest software (BD Biosciences, NJ, USA).

### **Clonogenic survival assay**

Cells were transfected with the indicated plasmids, siRNAs, miRNA mimics or inhibitors for 48 h, and then the cells were trypsinized and treated with cisplatin at the indicated doses for 2 h. The cells were then further cultured in 6 well plates with 500 cells/well for 2 weeks for the SGC7901 and BGC823 cells or 3 weeks for the SGC7901/DDP and BGC-823/DDP cells. For scoring colonies, the cells were fixed in 1 ml methanol for 15 min and stained with Giemsa for 10 min. The number of colonies was quantified, and each colony containing > 50 was counted.

### **Organoid culture**

This study was first approved by the Institutional Review Board of Nanjing Drum Tower Hospital. The standard procedure for organoid culture has been described previously [61]. Briefly, approximately 1 cm<sup>2</sup> of GC tumour tissues from cisplatin-resistant GC patients was isolated and the organoids were generated. Approximately 1 cm<sup>2</sup> of GC tissues from the cisplatin-resistant GC patient was minced, placed in a 10 cm Petri dish, covered with cold 1× chelating buffer (5.6 mM Na<sub>2</sub>HPO<sub>4</sub>, 8.0 mM KH<sub>2</sub>PO<sub>4</sub>, 96.2 mM NaCl, 1.6 mM KCl, 43.4 mM sucrose, 54.9 mM D-sorbitol, and 0.5 mM DL-dithiothreitol (pH = 7)), and cut into 20–50 small pieces of approximately 2–5 mm<sup>2</sup> in size. A glass microscopy slide was placed on top of the tissue pieces and pressed, and 10 ml of cold basal medium (Advanced DMEM/F12 supplemented with HEPES, Glutamax and 1× Primocin) was then added. The samples were centrifuged for 5 min at 200 × g and 4°C. The supernatant was discarded, and approximately 100 glands per 50 µl of basement matrix were seeded in one well of a 24-well plate warmed to 37°C. The plate was carefully transferred back to the cell culture incubator, and 500 µl of medium containing all growth factors (50 ng/ml EGF, 100 ng/ml noggin, 1 µg/ml R-spondin1, 50% Wnt-conditioned medium, 200 ng/ml FGF10, 1 nM gastrin, 2 µM TGF-beta inhibitor and 10 µM RHOKi) was carefully added to each well without disturbing the basement matrix. The medium was refreshed 3 times per week. After the organoids formed, they were minced into pieces, redigested, and transfected with CRAL, miR-505 overexpression or the corresponding control lentiviral vectors for 8 h. Then, the organoids were seeded into 24-well plates for 2 weeks with or without cisplatin (5 µg/ml), and organoid images were acquired with a Leica DMI8 system.

## Statistical analysis

Data in the graphs were generated from at least three independent experiments and are expressed as the mean  $\pm$  SD as indicated. The data were subjected to Student's *t* test (two-tailed, with  $P < 0.05$  considered significant) for simple comparison of two groups. The correlation of the expression of CRAL, miR-505 and CYLD was established by Pearson's correlation analysis. For Kaplan-Meier survival analysis, the expression of CRAL, miR-505 and CYLD was treated as a binary variant and was divided into 'high' and 'low' levels. The 25th percentile of CRAL expression was used as the cut-off value. All statistical tests were performed with the statistical analysis software IBM SPSS Statistics 20 (International Business Machines Corporation, New York, NY).

## Disclosure statement

No potential conflict of interest was reported by the authors.

## Funding

This work was supported in part by the National Natural Science Foundation of China (81773383, 81370078 to SYW; 81903085 to QW); and the Science Foundation for Distinguished Young Scholars of Jiangsu Province (BK20170047 to SYW); and the Fundamental Research Funds for the Central Universities (021414380439 to SYW); and the Foundation of Priority Academic Program Development (PAPD); and Postgraduate Research & Practice Innovation Program of Jiangsu Province (KYCX17\_1294 to ZRJ); and the United Fund of Nanjing Medical University and Southeast University to SYW and NL; and the Project funded by China Postdoctoral Science Foundation (2019M651808) to QW.

## References

- Bray F, Ferlay J, Soerjomataram I, et al. Global cancer statistics 2018: GLOBOCAN estimates of incidence and mortality worldwide for 36 cancers in 185 countries. *CA Cancer J Clin.* **2018**;68(6):394–424. PubMed PMID:30207593.
- Chen W, Sun K, Zheng R, et al. Cancer incidence and mortality in China, 2014. *Chin J Cancer Res.* **2018**;30(1):1–12. PubMed PMID:29545714;PubMed Central PMCID:PMC5842223.
- Fitzmaurice C, Allen C, Barber RM, Global Burden of Disease Cancer, C, et al. Global, regional, and national cancer incidence, mortality, years of life lost, years lived with disability, and disability-adjusted life-years for 32 cancer groups, 1990 to 2015: A systematic analysis for the global burden of disease study. *JAMA Oncol.* **2017**;3(4):524–548. PubMed PMID:27918777; PubMed Central PMCID:PMC6103527.
- Lipinska N, Romaniuk A, Paszel-Jaworska A, et al. Telomerase and drug resistance in cancer. *Cell Mol Life Sci.* **2017**;74(22):4121–4132. PubMed PMID:28623509;PubMed Central PMCID:PMC5641272.
- Shibue T, Weinberg RA. EMT, CSCs, and drug resistance: the mechanistic link and clinical implications. *Nat Rev Clin Oncol.* **2017**;14(10):611–629. PubMed PMID:28397828;PubMed Central PMCID:PMC5720366.
- Gottesman MM, Lavi O, Hall MD, et al. Toward a better understanding of the complexity of cancer drug resistance. *Annu Rev Pharmacol Toxicol.* **2016**;56:85–102. PubMed PMID:26514196.
- Konieczkowski DJ, Johannessen CM, Garraway LA. A convergence-based framework for cancer drug resistance. *Cancer Cell.* **2018**;33(5):801–815. PubMed PMID:29763622;PubMed Central PMCID:PMC5957297.
- Galluzzi L, Senovilla L, Vitale I, et al. Molecular mechanisms of cisplatin resistance. *Oncogene.* **2012**;31(15):1869–1883. PubMed PMID:21892204.
- Dogliotti G, Kullmann L, Dhumale P, et al. Membrane-binding and activation of LKB1 by phosphatidic acid is essential for development and tumour suppression. *Nat Commun.* **2017**;8:15747. PubMed PMID:28649994;PubMed Central PMCID:PMC5490199.
- Chen ZZ, Huang L, Wu Y-H, et al. LncSox4 promotes the self-renewal of liver tumour-initiating cells through Stat3-mediated Sox4 expression. *Nat Commun.* **2016**;7:12598. PubMed PMID:27553854;PubMed Central PMCID:PMC4999516.
- Mattick JS, Rinn JL. Discovery and annotation of long noncoding RNAs. *Nat Struct Mol Biol.* **2015**;22(1):5–7. PubMed PMID:25565026.
- Orom UA, Shiekhattar R. Long noncoding RNAs usher in a new era in the biology of enhancers. *Cell.* **2013**;154(6):1190–1193. PubMed PMID:24034243;PubMed Central PMCID:PMC4108076.
- Morris KV, Mattick JS. The rise of regulatory RNA. *Nat Rev Genet.* **2014**;15(6):423–437. PubMed PMID:24776770;PubMed Central PMCID:PMC4314111.
- Li RK, Gao J, Guo L-H, et al. PTENP1 acts as a ceRNA to regulate PTEN by sponging miR-19b and explores the biological role of PTENP1 in breast cancer. *Cancer Gene Ther.* **2017**;24(7):309–315. PubMed PMID:28731027.
- Liang L, Xu J, Wang M, et al. LncRNA HCP5 promotes follicular thyroid carcinoma progression via miRNAs sponge. *Cell Death Dis.* **2018**;9(3):372. PubMed PMID:29515098;PubMed Central PMCID:PMC5841368.
- Wang Y, Zhang L, Zheng X, et al. Long non-coding RNA LINC00161 sensitises osteosarcoma cells to cisplatin-induced apoptosis by regulating the miR-645-IFIT2 axis. *Cancer Lett.* **2016**;382(2):137–146. PubMed PMID:27609068.
- Kumar MS, Armenteros-Monterroso E, East P, et al. HMGA2 functions as a competing endogenous RNA to promote lung cancer progression. *Nature.* **2014**;505(7482):212–217. PubMed PMID:24305048;PubMed Central PMCID:PMC3886898.
- Qu L, Ding J, Chen C, et al. Exosome-transmitted lncARSR promotes sunitinib resistance in renal cancer by acting as a competing endogenous RNA. *Cancer Cell.* **2016**;29(5):653–668. PubMed PMID:27117758.
- Tang J, Zhuo H, Zhang X, et al. A novel biomarker Linc00974 interacting with KRT19 promotes proliferation and metastasis in hepatocellular carcinoma. *Cell Death Dis.* **2014**;5:e1549. PubMed PMID:25476897;PubMed Central PMCID:PMC4649834.
- Xu W, Chen Q, Wang Q, et al. JWA reverses cisplatin resistance via the CK2-XRCC1 pathway in human gastric cancer cells. *Cell Death Dis.* **2014**;5:e1551. PubMed PMID:25476899;PubMed Central PMCID:PMC4649833.
- Wu XS, Wang F, Li H-F, et al. LncRNA-PAGBC acts as a microRNA sponge and promotes gallbladder tumorigenesis. *EMBO Rep.* **2017**;18(10):1837–1853. PubMed PMID:28887321; PubMed Central PMCID:PMC5623869.
- Noh JH, Kim KM, McClusky WG, et al. Cytoplasmic functions of long noncoding RNAs. *Wiley Interdiscip Rev RNA.* **2018**. PubMed PMID:29516680. DOI:10.1002/wrna.1471.
- Liu XH, Sun M, Nie F-Q, et al. Lnc RNA HOTAIR functions as a competing endogenous RNA to regulate HER2 expression by sponging miR-331-3p in gastric cancer. *Mol Cancer.* **2014**;13:92. PubMed PMID:24775712;PubMed Central PMCID:PMC4021402.
- Jia J, Zhan D, Li J, et al. The contrary functions of lncRNA HOTAIR/miR-17-5p/PTEN axis and Shenqifuzheng injection on chemosensitivity of gastric cancer cells. *J Cell Mol Med.* **2019**;23(1):656–669. PubMed PMID:30338929;PubMed Central PMCID:PMC6307763.
- Li Y, Wu Z, Yuan J, et al. Long non-coding RNA MALAT1 promotes gastric cancer tumorigenicity and metastasis by regulating vasculogenic mimicry and angiogenesis. *Cancer Lett.* **2017**;395:31–44. PubMed PMID:28268166.

- [26] Mishra S, Verma SS, Rai V, et al. Long non-coding RNAs are emerging targets of phytochemicals for cancer and other chronic diseases. *Cell Mol Life Sci.* **2019**;76(10):1947–1966. PubMed PMID:30879091.
- [27] Xi Z, Si J, Nan J. LncRNA MALAT1 potentiates autophagy-associated cisplatin resistance by regulating the microRNA30b/autophagy-related gene 5 axis in gastric cancer. *Int J Oncol.* **2019**;54(1):239–248. PubMed PMID:30365113.
- [28] Frank CG, Reguerio V, Rother M, et al. *Klebsiella pneumoniae* targets an EGF receptor-dependent pathway to subvert inflammation. *Cell Microbiol.* **2013**;15(7):1212–1233. PubMed PMID:23347154.
- [29] Yang WL, Jin G, Li C-F, et al. Cycles of ubiquitination and deubiquitination critically regulate growth factor-mediated activation of Akt signaling. *Sci Signal.* **2013**;6(257):ra3. PubMed PMID:23300340;PubMed Central PMCID:PMC3862898.
- [30] Urbanik T, Koehler BC, Wolpert L, et al. CYLD deletion triggers nuclear factor-kappaB-signaling and increases cell death resistance in murine hepatocytes. *World J Gastroenterol.* **2014**;20(45):17049–17064. PubMed PMID:25493017;PubMed Central PMCID:PMC4258573.
- [31] Zhu M, Zhou X, Du Y, et al. miR-20a induces cisplatin resistance of a human gastric cancer cell line via targeting CYLD. *Mol Med Rep.* **2016**;14(2):1742–1750. PubMed PMID:27357419.
- [32] Oshimori N, Oristian D, Fuchs E. TGF-beta promotes heterogeneity and drug resistance in squamous cell carcinoma. *Cell.* **2015**;160(5):963–976. PubMed PMID:25723170;PubMed Central PMCID:PMC4509607.
- [33] Wang X, Arai S, Song X, et al. Induced ncRNAs allosterically modify RNA-binding proteins in cis to inhibit transcription. *Nature.* **2008**;454(7200):126–130. PubMed PMID:18509338;PubMed Central PMCID:PMC2823488.
- [34] Wang KC, Yang YW, Liu B, et al. A long noncoding RNA maintains active chromatin to coordinate homeotic gene expression. *Nature.* **2011**;472(7341):120–124. PubMed PMID:21423168;PubMed Central PMCID:PMC3670758.
- [35] Abdollahzadeh R, Daraei A, Mansoori Y, et al. Competing endogenous RNA (ceRNA) cross talk and language in ceRNA regulatory networks: A new look at hallmarks of breast cancer. *J Cell Physiol.* **2019**;234(7):10080–10100. PubMed PMID:30537129.
- [36] Qi X, Zhang D-H, Wu N, et al. ceRNA in cancer: possible functions and clinical implications. *J Med Genet.* **2015**;52(10):710–718. PubMed PMID:26358722.
- [37] Tan X, Banerjee P, Liu X, et al. The epithelial-to-mesenchymal transition activator ZEB1 initiates a prometastatic competing endogenous RNA network. *J Clin Invest.* **2018**. PubMed PMID:29324442. DOI:10.1172/JCI97225.
- [38] Cao C, Zhang T, Zhang D, et al. The long non-coding RNA, SNHG6-003, functions as a competing endogenous RNA to promote the progression of hepatocellular carcinoma. *Oncogene.* **2017**;36(8):1112–1122. PubMed PMID:27530352.
- [39] Zhuang J, Shen L, Yang L, et al. TGFbeta1 promotes gemcitabine resistance through regulating the LncRNA-LET/NF90/miR-145 signaling axis in bladder cancer. *Theranostics.* **2017**;7(12):3053–3067. PubMed PMID:28839463;PubMed Central PMCID:PMC5566105.
- [40] Cui H, Zhang Y, Zhang Q, et al. A comprehensive genome-wide analysis of long noncoding RNA expression profile in hepatocellular carcinoma. *Cancer Med.* **2017**;6(12):2932–2941. PubMed PMID:29047230;PubMed Central PMCID:PMC5727245.
- [41] Shen J, Siegel AB, Remotti H, et al. Identifying microRNA panels specifically associated with hepatocellular carcinoma and its different etiologies. *Hepatoma Res.* **2016**;2:151–162. PubMed PMID:28243631;PubMed Central PMCID:PMC5325160.
- [42] Yamamoto Y, Yoshioka Y, Minoura K, et al. An integrative genomic analysis revealed the relevance of microRNA and gene expression for drug-resistance in human breast cancer cells. *Mol Cancer.* **2011**;10:135. PubMed PMID:22051041;PubMed Central PMCID:PMC3247093.
- [43] Dang SC, Wang F, Qian X-B, et al. MicroRNA-505 suppresses gastric cancer cell proliferation and invasion by directly targeting Polo-like kinase-1. *Onco Targets Ther.* **2019**;12:795–803. PubMed PMID:30774367;PubMed Central PMCID:PMC6352865.
- [44] Chen Y, Bian L, Zhang Y. MiR-505 mediates methotrexate resistance in colorectal cancer by targeting RASSF8. *J Pharm Pharmacol.* **2018**;70(7):937–951. PubMed PMID:29726011.
- [45] Bissierier M, Wajapeyee N. Mechanisms of resistance to EZH2 inhibitors in diffuse large B-cell lymphomas. *Blood.* **2018**. PubMed PMID:29572378. DOI:10.1182/blood-2017-08-804344.
- [46] Wicki A, Mandalà M, Massi D, et al. Acquired resistance to clinical cancer therapy: a twist in physiological signaling. *Physiol Rev.* **2016**;96(3):805–829. PubMed PMID:27142452.
- [47] Tripathi SC, Fahrman JF, Celiktas M, et al. MCAM mediates chemoresistance in small-cell lung cancer via the PI3K/AKT/SOX2 signaling pathway. *Cancer Res.* **2017**;77(16):4414–4425. PubMed PMID:28646020.
- [48] Mercado-Lubo R, Zhang Y, Zhao L, et al. A Salmonella nanoparticle mimic overcomes multidrug resistance in tumours. *Nat Commun.* **2016**;7:12225. PubMed PMID:27452236;PubMed Central PMCID:PMC5512628.
- [49] Ma Y, Yang Y, Wang F, et al. Long non-coding RNA CCAL regulates colorectal cancer progression by activating Wnt/beta-catenin signalling pathway via suppression of activator protein 2alpha. *Gut.* **2016**;65(9):1494–1504. PubMed PMID:25994219.
- [50] Soriano GP, Besse L, Li N, et al. Proteasome inhibitor-adapted myeloma cells are largely independent from proteasome activity and show complex proteomic changes, in particular in redox and energy metabolism. *Leukemia.* **2016** 11;30:2198–2207. PubMed PMID:27118406;PubMed Central PMCID:PMC5097071.
- [51] Ji YX, Huang Z, Yang X, et al. The deubiquitinating enzyme cylindromatosis mitigates nonalcoholic steatohepatitis. *Nat Med.* **2018**;24(2):213–223. PubMed PMID:29291351.
- [52] Rajan N, Ashworth A. Inherited cylindromas: lessons from a rare tumour. *Lancet Oncol.* **2015**;16(9):e460–e469. PubMed PMID:26370355.
- [53] Nikolaou K, Tsagaratou A, Eftychi C, et al. Inactivation of the deubiquitinase CYLD in hepatocytes causes apoptosis, inflammation, fibrosis, and cancer. *Cancer Cell.* **2012**;21(6):738–750. PubMed PMID:22698400.
- [54] Kupka S, De Miguel D, Draber P, et al. SPATA2-mediated binding of CYLD to HOIP enables CYLD recruitment to signaling complexes. *Cell Rep.* **2016**;16(9):2271–2280. PubMed PMID:27545878;PubMed Central PMCID:PMC5009064.
- [55] van Andel H, Kocemba KA, de Haan-kramer A, et al. Loss of CYLD expression unleashes Wnt signaling in multiple myeloma and is associated with aggressive disease. *Oncogene.* **2017**;36(15):2105–2115. PubMed PMID:27775078.
- [56] Obenaus AC, Zou Y, Ji AL, et al. Therapy-induced tumour secretomes promote resistance and tumour progression. *Nature.* **2015**;520(7547):368–372. PubMed PMID:25807485;PubMed Central PMCID:PMC4507807.
- [57] Mayer IA, Arteaga CL. The PI3K/AKT pathway as a target for cancer treatment. *Annu Rev Med.* **2016**;67:11–28. PubMed PMID:26473415.
- [58] Oki Y, Fanale M, Romaguera J, et al. Phase II study of an AKT inhibitor MK2206 in patients with relapsed or refractory lymphoma. *Br J Haematol.* **2015**;171(4):463–470. PubMed PMID:26213141;PubMed Central PMCID:PMC5278973.
- [59] Xu W, Wang S, Chen Q, et al. TXNL1-XRCC1 pathway regulates cisplatin-induced cell death and contributes to resistance in human gastric cancer. *Cell Death Dis.* **2014**;5:e1055. PubMed PMID:24525731;PubMed Central PMCID:3944244.
- [60] Wang S, Wu X, Zhang J, et al. CHIP functions as a novel suppressor of tumour angiogenesis with prognostic significance in human gastric cancer. *Gut.* **2013**;62(4):496–508. PubMed PMID:22535373.
- [61] McCracken KW, Catá EM, Crawford CM, et al. Modelling human development and disease in pluripotent stem-cell-derived gastric organoids. *Nature.* **2014**;516(7531):400–404. PubMed PMID:25363776;PubMed Central PMCID:PMC4270898.